

NOTICE: this is the author's version of a work that was accepted for publication in Planetary and Space Science. Changes resulting from the publishing process, such as peer review, editing, corrections, structural formatting, and other quality control mechanisms may not be reflected in this document. Changes may have been made to this work since it was submitted for publication. A definitive version was subsequently published in Planetary and Space Science, Vol. 90 (2014). DOI: 10.1016/j.pss.2013.11.003

1  
2  
3  
4  
5  
6  
7  
8  
9  
10 Silence on Shangri-La : Detection of Titan Surface Volatiles by Acoustic  
11  
12  
13 Absorption in Huygens Probe Measurements  
14  
15  
16  
17  
18  
19  
20  
21  
22  
23

24 Ralph D. Lorenz\*, Johns Hopkins University Applied Physics Laboratory, Laurel, MD 20723, USA  
25

26  
27  
28 Mark R. Leese, Brijen Hathi, John C. Zarnecki, Axel Hagermann, The Open University, Milton  
29  
30  
31 Keynes, UK  
32

33  
34 Phil Rosenberg, University of Leeds, Leeds, UK  
35  
36

37  
38 Martin C. Towner, Department of Applied Geology, Curtin University, Perth, Australia  
39

40  
41 James Garry, Red Core Consulting, Burnaby, British Columbia, Canada  
42

43  
44 Håkan Svedhem, European Space Agency, ESTEC, Noordwijk, The Netherlands  
45  
46  
47  
48  
49

50  
51 Submitted to Planetary and Space Science, July 23, 2013  
52

53  
54  
55 \* corresponding author. Tel. +1 443 778 2903 Fax. +1 443 778 8939 ralph.lorenz@jhuapl.edu  
56  
57  
58  
59  
60  
61  
62  
63  
64  
65

1  
2  
3  
4  
5  
6  
7  
8  
9 Objective:

10  
11  
12 Characterize and understand acoustic instrument performance on the surface of Titan  
13  
14

15  
16 Methods:

17  
18  
19 The Huygens probe measured the speed of sound in Titan's atmosphere with a 1MHz pulse  
20  
21  
22 time-of-flight transducer pair near the bottom of the vehicle. We examine the fraction of  
23  
24  
25 pulses correctly received as a function of time.  
26

27  
28 Results :

29  
30  
31 This system returned good data from about 11km altitude, where the air became thick enough  
32  
33  
34 to effectively transmit the sound, down to the surface just before landing : these data have  
35  
36  
37 been analyzed previously. After an initial transient at landing, the instrument operated  
38  
39  
40 nominally for about 10 minutes, recording pulses much as during descent. The fraction of  
41  
42  
43 pulses detected then declined and the transmitted sound ceased to be detected altogether,  
44  
45  
46 despite no indication of instrument or probe configuration changes.  
47  
48  
49

50  
51 Conclusions:

52  
53  
54  
55 The most likely explanation appears to be absorption of the signal by polyatomic gases with  
56  
57  
58 relaxation losses at the instrument frequency, such as ethane, acetylene and carbon dioxide.  
59

60 These vapors, detected independently by the GCMS instrument, were evolved from the surface  
61  
62  
63  
64  
65

1  
2  
3  
4  
5 material by the warmth leaking from the probe, and confirm the nature of the surface materials  
6  
7  
8 as 'damp' with a cocktail of volatile compounds. Some suggestions for future missions are  
9  
10 considered.  
11  
12  
13  
14  
15  
16  
17

18 Practice Implications :

19  
20  
21 None.  
22  
23

24 Keywords : Instrumentation ; Acoustics ; Planetary Atmospheres ; Organic Chemistry ;

25  
26  
27 Attenuation ; Huygens Probe  
28  
29  
30  
31  
32  
33  
34  
35  
36  
37  
38  
39  
40  
41  
42  
43  
44  
45  
46  
47  
48  
49  
50  
51  
52  
53  
54  
55  
56  
57  
58  
59  
60  
61  
62  
63  
64  
65

## 1. Introduction

Titan is unique among the satellites of the solar system in that it has an atmosphere. This makes it of particular interest to acousticians (e.g. Leighton and White, 2005; Leighton and Petculescu, 2009) since the propagation of sound is of interest in its own right, both for education/outreach as well as for science, as well as serving as a means to study winds and transient phenomena such as precipitation, wave breaking, thunder, volcanic eruptions and bolide entry. Titan's thick atmosphere is favorable for the generation and receipt of soundwaves by transducers, and the low temperatures make the attenuation by the constituent gases relatively low(e.g. Petcelescu and Lueptow, 2007; Hanford et al., 2009).

Although the Cassini spacecraft in Saturn orbit continues to make remarkable findings at Titan and motivates future in-situ exploration by landers, balloons or other platforms, the only available in-situ environmental data from Titan's surface is that from the Huygens probe, from which data were received for 72 minutes after its landing at the western margins of the Shangri-La dunefields near Titan's equator. It is therefore important to examine these data, hard-won from Titan's cryogenic environment, for whatever insights they may offer - even when the data were not necessarily acquired through the expected operation of the relevant instrumentation. Since a number of proposed future investigations have considered ultrasonic anemometers, depth sounders, and passive microphones, we therefore examine the surface operation of the Huygens acoustic instrumentation, whose results were not interpreted previously.

1  
2  
3  
4  
5  
6 The Huygens probe to Titan carried three acoustic instruments. A passive microphone, part of  
7  
8 the Huygens Atmospheric Structure Instrument (HASI) was intended to search for thunder, but  
9  
10 detected only aeroacoustic noise during descent. The Surface Science Package (SSP) carried a  
11  
12 down-pointing sonar, the Acoustic Properties Instrument - Sounder (API-S) which detected an  
13  
14 echo from the surface during the last seconds of parachute descent (Zarnecki et al., 2005;  
15  
16 Towner et al., 2007), and a speed-of-sound sensor (Acoustic Properties Instrument - Velocity, or  
17  
18 API-V). It is this latter instrument that forms the topic of the present paper.  
19  
20  
21  
22  
23  
24  
25  
26  
27

## 28 2. Instrumentation

29  
30  
31 When the Huygens probe was conceived, a prevailing model for Titan's surface was of a global  
32  
33 ocean and, while post-landing survival was not guaranteed, the possibility of making brief  
34  
35 measurements on the surface was recognized. The probe specification demanded that it float,  
36  
37 and that the battery energy and communications budgets permit at least 3 minutes of surface  
38  
39 operations. One quick measurement that was included as a diagnostic of the methane:ethane  
40  
41 ratio in the ocean was a speed of sound measurement, implemented within the Surface Science  
42  
43 Package (SSP) on the probe (Zarnecki et al., 1997). This measurement (as others such as  
44  
45 dielectric constant and refractive index in the SSP) required sensors to be immersed in the  
46  
47 ocean, and so these were mounted near the apex of the probe (figure 1).  
48  
49  
50  
51  
52  
53  
54  
55  
56  
57  
58

59 < Figure 1 >  
60  
61  
62  
63  
64  
65

1  
2  
3  
4  
5  
6  
7  
8  
9 The speed of sound measurement on Huygens was very simple in concept : a pair of  
10 transducers are separated by a known distance (12.7cm), and the propagation time of a pulse  
11 of ultrasound (1MHz) across that distance is measured by starting a clock on emission at one  
12 transducer and stopping it on receipt at the other. In practice (e.g. Rosenberg 2008;  
13 Hagermann et al., 2007) the simple design using a threshold detector on the receive circuit led  
14 to some subtleties in performance.  
15  
16  
17  
18  
19  
20  
21  
22  
23  
24

25 The principal objective of the measurement was to diagnose liquid composition, and to provide  
26 a sound speed to permit the echo delay time from a small acoustic depth-sounder to be  
27 interpreted as an ocean depth. During development it was realized that meaningful data might  
28 also be obtained during descent (e.g. Lorenz, 1994; Garry, 1996; Zarnecki et al., 1997; Svedhem  
29 et al., 2004 ).  
30  
31  
32  
33  
34  
35  
36  
37  
38  
39  
40

41 The instrument consisted of two sensor heads (API-V1 and API-V2) each containing a  
42 piezoelectric element (PXE-5) able to act as both a transmitter and a receiver. The sensor heads  
43 were mounted opposite and facing each other across the SSP cavity (figure 2) allowing  
44 atmospheric gases to flow past them. The sensors were mounted at the opening of the cavity,  
45 but behind an electromagnetic shield (figure 3) designed to prevent damage to the  
46 instrumentation from any lightning or electrostatic discharge.  
47  
48  
49  
50  
51  
52  
53  
54  
55  
56  
57  
58  
59  
60  
61  
62  
63  
64  
65

1  
2  
3  
4  
5 To make a measurement, a 1-MHz wavetrain of nominally 10  $\mu\text{s}$  duration (i.e. 10 cycles) was  
6 transmitted between the sensors and the time of flight of this sound wave was measured. The  
7  
8 timing clock had a frequency of 4 MHz giving a time resolution for the measurement of 0.25  $\mu\text{s}$ .  
9  
10  
11 This process was repeated twice per second (once in each direction) potentially providing  
12  
13  
14 metre-scale vertical resolution during the descent through Titan's atmosphere.  
15  
16  
17  
18  
19  
20

21 Experimentation with flight spare sensors revealed that it takes a time  $t_0 = 3.71 \mu\text{s}$  for the  
22  
23 sound waves to propagate out of the transmitting sensor and into the receiving sensor,  
24  
25 assuming zero free-space separation. It is clear that this value of  $t_0$  is determined by the  
26  
27 capacitance of the piezoelectric crystals as well as the thickness of, and speed of sound within,  
28  
29 the crystals and their impedance matching coatings.  
30  
31  
32  
33  
34  
35

36 Experimentation with flight spare sensors also revealed that the envelope of the received signal  
37  
38 is more bell shaped than the transmitted signal. This effect, due to the resonant response of the  
39  
40 transducer with finite  $Q$ , means that early peaks in the signal train may not have large enough  
41  
42 amplitude to be detected. Each peak missed in this way causes API-V to overestimate the time  
43  
44 of flight by 1  $\mu\text{s}$ . Before encounter it was expected that, as the probe descended and the  
45  
46 density of the atmosphere increased, the received signal would become stronger and fewer  
47  
48 peaks would be missed in this way. This would manifest itself in the flight data in the form of  
49  
50 discontinuities separated by 1  $\mu\text{s}$  in a plot of time of flight vs altitude.  
51  
52  
53  
54  
55  
56  
57  
58  
59  
60  
61  
62  
63  
64  
65



1  
2  
3  
4  
5  
6 Given the trigger voltage threshold on the flight sensor of 69.9 mV, operation was expected to  
7  
8 require a transmission coefficient of at least  $\sim 0.315 \times 10^{-3}$  which, using room temperature data  
9  
10 for the sensor materials, corresponds to a required impedance of the sampled gas of at least  
11  
12  $\sim 629$  Rayl. Examining the predicted engineering model for Titan's atmosphere, it should have  
13  
14  $\sim 629$  Rayl. Examining the predicted engineering model for Titan's atmosphere, it should have  
15  
16 been expected that the sensor would begin to operate at around 10-12 km altitude.  
17  
18  
19  
20  
21  
22

23  
24 < Figure 2 >  
25  
26  
27  
28  
29

30  
31 < Figure 3  
32  
33

### 34 3. Data

35  
36  
37

38 The data analyzed here are the propagation times measured by the API-V instrument during the  
39  
40 descent, as calibrated and archived on the NASA Planetary Data System (PDS). The data are in  
41  
42 the Huygens SSP archive maintained on the PDS Atmospheres Node at New Mexico State  
43  
44 University (presently,  
45  
46 [http://atmos.pds.nasa.gov/data\\_and\\_services/atmospheres\\_data/Huygens/SSP.html](http://atmos.pds.nasa.gov/data_and_services/atmospheres_data/Huygens/SSP.html)) and are  
47  
48 mirrored on the European Space Agency Planetary Science Archive (PSA) . The data (filename  
49  
50 SSP\_APIV\_123456\_0\_R\_ATMOS.TAB) comprise a tabulation of sample times relative to the  
51  
52 spacecraft reference T0 (the firing of the parachute mortar at the end of the hypersonic entry  
53  
54 into the atmosphere), an instrument mode flag and record number, and the two times for  
55  
56  
57  
58  
59  
60  
61  
62  
63  
64  
65

1  
2  
3  
4  
5 propagation of the sound pulse in each direction, expressed in the raw digital counter number,  
6  
7  
8 and as a time in milliseconds. Documentation of the data is in the PDS data label file  
9  
10  
11 SSP\_APIV\_123456\_0\_R\_ATMOS.LBL and the calibration file SSP\_CAL.ASC.  
12

13  
14 The latter file notes that the distance between the two transducer faces is 0.1289m, and that  
15  
16 the digital counter number refers to a 4 MHz clock. As discussed in the text above and in  
17  
18 Hagermann et al. (2007), there is a ~3.7 us offset to account for the propagation out of and into  
19  
20  
21 the transducers.  
22  
23  
24  
25  
26  
27  
28  
29  
30  
31  
32  
33  
34  
35

36 < Figure 4 >  
37  
38  
39  
40  
41

42 Figure 4 shows the recorded API-V dataset taken during Huygens descent. Although API-V was  
43  
44 switched on only 600 s after initial parachute deployment, the upper atmosphere was too  
45  
46 tenuous for sufficient atmosphere–sensor coupling and the first successful measurement  
47  
48 occurred at an altitude of just above 11 km. It can be seen that speed of sound decreases with  
49  
50 altitude, an effect caused mostly by the associated decrease in temperature. There is also a  
51  
52 spread of approximately  $3 \text{ ms}^{-1}$ , much larger than the expected absolute accuracy of the  
53  
54 sensors of  $0.3 \text{ ms}^{-1}$  based upon the accuracy of measuring the time of flight and the sensor  
55  
56 separation. This spread of data has been studied by taking the difference between the  
57  
58  
59  
60  
61  
62  
63  
64  
65

1  
2  
3  
4  
5 measured time of flight and the value expected for pure nitrogen for all measurements taken  
6  
7  
8 below 6 km. A random number of peaks is seen during each measurement instead of simply  
9  
10  
11 missing fewer as the pressure increases. The effect is much reduced on the surface with a  
12  
13 spread of less than  $1 \text{ ms}^{-1}$ . Turbulent eddies passing between the sensors during descent might  
14  
15  
16 have caused a seemingly random change of the scattering properties of the gas, creating this  
17  
18 effect. This means that each data point can be considered a lower limit on the speed of sound  
19  
20  
21 with a relative resolution better than  $7.5 \text{ cm s}^{-1}$  based on the  $0.25 \mu\text{s}$  sampling rate; but the  
22  
23  
24 absolute speed of sound could be higher by integer multiples of  $\sim 30 \text{ cm s}^{-1}$ , based on the 1-  
25  
26 MHz pulse frequency.  
27  
28  
29  
30  
31

### 32 3.1 Descent Timeouts and Spurious Early Triggers

33  
34  
35 In order to obtain a high altitude resolution, e.g. to characterize the planetary boundary layer,  
36  
37  
38 measurements are made once every second. Although it was only expected that the acoustic  
39  
40  
41 impedance of the atmosphere would become large enough to reliably detect the transmitted  
42  
43  
44 pulse towards the end of descent (when the atmosphere would be about 1000 times denser  
45  
46 than at the start) measurements began at the beginning of descent.  
47  
48  
49

50 A small variation in the actual value of the timeout clock timer is presumably related to  
51  
52 parametric drift in the timer components : the SSP electronics temperatures (e.g. Leese et al.,  
53  
54  
55 2012) show a time history very similar to the envelope of the timeouts, with a small increase  
56  
57  
58 from the beginning until about 3000s, and a slow decline thereafter. The expected timeouts  
59  
60  
61 were observed through time 1571s, when T1 triggers early, and then more frequently through  
62  
63  
64  
65

1  
2  
3  
4  
5  
6 ~1844s, when T2 also triggers early. Early triggers are then seen, often in bursts, on both  
7  
8 channels and in fact more often on T2, until at about 4700s they cease and timeouts resume  
9  
10 consistently.  
11

12  
13  
14 It is tempting to associate these anomalous early triggers with the cause of noise seen on the  
15  
16 sounder instrument which we know to be due to the operation of a high speed pump on the  
17  
18 Aerosol Collector/Pyrolyzer instrument (see the pump current and speed history in  
19  
20 housekeeping data archived at  
21  
22 [http://atmos.nmsu.edu/PDS/data/hpacp\\_0001/DATA/ACP\\_PUMP\\_V1\\_0.TAB](http://atmos.nmsu.edu/PDS/data/hpacp_0001/DATA/ACP_PUMP_V1_0.TAB)). This fan  
23  
24 operated at around 25000 rpm from 1500s until 3500s, and 4650-5310s. Thus the  
25  
26 correspondence of the API-V triggers is far from complete and another explanation must be  
27  
28 sought for at least some of the triggers. It seems likely that some kind of turbulence or  
29  
30 aeroacoustic effect may have been responsible. Most curiously, when the instrument appears  
31  
32 to be operating nominally in the lower atmosphere (where the dense gas allows good coupling  
33  
34 and thus a strong signal) T1 again triggers early at 7767s (at about 5km altitude), then again at  
35  
36 7870s, and with increasing frequency through ~8000s where it triggers most of the time until  
37  
38 landing at 8870s.  
39  
40  
41  
42  
43  
44  
45  
46  
47

48 Some support for an aerodynamic explanation derives from the fact that no early triggers  
49  
50 occurred after landing. Furthermore, the motions of the probe were recorded by  
51  
52 accelerometers and tilt sensors (e.g. Lorenz et al., 2007) which documented that the probe was  
53  
54 buffeted significantly prior to 5500s, but was fairly quiescent thereafter. Although ground tests  
55  
56 showed that the fairly narrow sound beam between the transducers can be scattered by  
57  
58  
59  
60  
61  
62  
63  
64  
65

1  
2  
3  
4  
5  
6 modest airflow (e.g. from a desk fan) which would lead to timeouts, turbulent airflow in the SSP  
7  
8 cavity seems unlikely to be the cause of early triggers, since flow through the instrument is  
9  
10 limited by a narrow vent tube, and the ESD grille (figure 3) would further suppress airflow  
11  
12  
13 fluctuations. Perhaps the most likely cause of early triggers is vibrations from structural flexing  
14  
15  
16 of the probe due to the turbulent motion in this period.  
17  
18  
19  
20  
21  
22

23 < Figure 5 >  
24  
25  
26  
27  
28

### 29 3.2 Post-Landing Suppression of Propagation 30 31 32 33 34 35

36 < Figure 6 >  
37  
38  
39

40 < Figure 7 >  
41  
42  
43  
44  
45  
46

47 The post-landing environment of the Huygens probe was very quiescent after the first ~6  
48  
49 seconds when there was some bouncing and skidding (Bettanini et al., 2007; Schroeder et al.,  
50  
51 2012). The orientation of the probe changed very slightly, with a tilt of ~0.2 degrees occurring  
52  
53 over 72 minutes (Karkoschka et al., 2007). The camera observed no other changes, apart from  
54  
55 a possible methane dewdrop forming on the camera baffle and falling through the field of view  
56  
57  
58  
59  
60 (Karkoschka and Tomasko, 2009) - this was observed on Image #897 which was acquired at  
61  
62  
63  
64  
65

1  
2  
3  
4  
5 T0+10,423s, i.e. 1553s after landing. Additionally, material either inside or immediately  
6  
7 adjacent to the heated inlet of the GCMS instrument progressively warmed up after landing  
8  
9 (Lorenz et al., 2006) evolved methane, and later ethane and some other compounds after  
10  
11 landing (Niemann et al., 2005, 2010). The thermal interactions of the warm - but well-insulated  
12  
13 and therefore cold-skinned - probe with the surface environment are discussed in Lorenz  
14  
15  
16  
17  
18 (2006).  
19  
20

21  
22  
23  
24  
25 Since no major temperature changes occurred, and no major change in position, some change  
26  
27 in the material around or between the transducers seems to have been responsible for the  
28  
29 drop in received signals. One hypothesis speculatively advanced in a thesis by Rosenberg (2007)  
30  
31 was that liquid from the damp subsurface seeped into the cavity made by the probe and  
32  
33 reduced the atmospheric coupling between the transducers by allowing some of the pulse  
34  
35 energy to propagate into the liquid and surface material. This scenario could be considered  
36  
37 under the paradigm that the probe penetrated into the ground, decelerating over a distance of  
38  
39 around 15cm (e.g. Zarnecki et al., 2005). However, understanding of the probe post-impact  
40  
41 motion has since improved (Schroeder et al., 2012), concluding that the probe bounced or  
42  
43 skidded out of this impact depression. There is evidence that the probe was left sitting on the  
44  
45 surface, rather than having penetrated into it (from the camera geometry, Karkoschka et al.,  
46  
47 2007, and from the multipath interference pattern observed in the Huygens radio signal, Perez-  
48  
49 Ayucar et al., 2006). Thus a liquid intrusion scenario seems unlikely.  
50  
51  
52  
53  
54  
55  
56  
57  
58  
59  
60  
61  
62  
63  
64  
65

1  
2  
3  
4  
5  
6 On the other hand, the introduction of heavier gases into the SSP cavity between the  
7  
8 transducers may have dramatically reduced the pulse strength. With small amounts of gas,  
9  
10 the sound speed would not be significantly affected, yet the attenuation at 1 MHz could be  
11  
12 substantially increased, as we note in the next section. It is seen in figure 4 that the post-  
13  
14 impact propagation times decrease slowly, as would be expected from either warming, or a  
15  
16 decrease in the relative molecular weight (due to an increasing methane concentration).  
17  
18 However, even assuming the temperature evolution of the instrument (see later) to be  
19  
20 representative of the acoustic cavity, the interpretation of the post-impact sound speed is not  
21  
22 unique, since higher molecular weight gases may have partially offset the methane abundance.  
23  
24  
25  
26  
27  
28  
29  
30  
31  
32

#### 33 4. Temperature Environment and Candidate Gas Evolution

34  
35  
36  
37  
38  
39

40 If we hypothesize that the nondetection of pulses post-landing is due to the introduction of an  
41  
42 attenuating gas into the SSP cavity, then we can use the descent data as a proxy calibration.  
43  
44 Specifically, for the absorber to cause the loss of signal, it must introduce an attenuation  
45  
46 equivalent to the difference in transmission between the unperturbed atmosphere at the  
47  
48 surface and the atmosphere at the altitude where a similarly low pulse detection rate was  
49  
50 encountered. Specifically, since the detection rate was near-zero at ~10km altitude, the  
51  
52 surface absorber must have attenuated the signal by a factor of  $\sim(\rho_{10}c_{10}/\rho_0c_0)^2$  or  
53  
54  $[(3.5*184)/(5.4*194)]^2 = 0.37$ , 1 neper (np) or 4.3dB. Thus the localized atmosphere in the SSP  
55  
56  
57  
58  
59  
60  
61  
62  
63  
64  
65

1  
2  
3  
4  
5  
6 cavity has an attenuation coefficient  $\alpha$  of  $4.3/0.12 \sim 40$  dB/m or  $\sim 8$  np/m : it is probable that  
7  
8 this aggregate attenuation is the result of the absorption by several different gas species  
9  
10 together, each at a modest concentration.  
11  
12

13  
14 Dain and Lueptow (2001) examine the attenuation in methane-air mixtures, showing that the  
15  
16 attenuation ( $\alpha\lambda$ ) at 600kHz/bar is substantially influenced by molecular relaxation of methane,  
17  
18 having  $\alpha\lambda \sim 0.01$  for high methane concentrations at 297K. For the wavelength of the Titan  
19  
20 experiment with  $c \sim 200$  m/s,  $\lambda \sim 0.2$ mm and thus  $\alpha \sim 50$  np/m for pure methane. The methane  
21  
22 concentration was measured (Niemann et al., 2005) to be  $\sim 5\%$  in the free atmosphere (where  
23  
24 of course the pulses were transmitted successfully), but it could have risen slightly in the SSP  
25  
26 cavity. Heavier gases which were essentially absent in the free atmosphere but which may  
27  
28 have accumulated in the warming cavity seem a more likely candidate to provide the  
29  
30 incremental attenuation. Ethane is a strong candidate (see later) but there are several others  
31  
32 (see figures 8 and 9) and it will not be possible to discriminate their contributions since  
33  
34 measurements at only one frequency were made.  
35  
36  
37  
38  
39  
40  
41  
42

43  
44 Martinsson and Delsing (2002) give measurements of the attenuation of (pure) ethane at  
45  
46 600kHz/bar (i.e. the condition of the 1MHz measurement at 1.5 bar) of 30-40 neper/m. The  
47  
48 corresponding attenuation of Carbon monoxide was  $\sim 10$  neper/m. Holmes et al. (1964) obtain  
49  
50 a similar value for ethane, and find propane to have an attenuation about a factor of 2 lower.  
51  
52  
53 All these data are at room temperature.  
54  
55  
56  
57  
58  
59  
60  
61  
62  
63  
64  
65



1  
2  
3  
4  
5  
6 < Figure 8 >  
7

8  
9 < Figure 9 >  
10

11  
12  
13  
14  
15  
16 The quantitative interpretation of the Huygens measurement really requires low-temperature  
17  
18 attenuation measurements which are not, as far as the authors are aware, available. The  
19  
20 actual gas mixture that formed in the acoustic cavity on Huygens cannot in any case be uniquely  
21  
22 determined : our only intent here is to show that methane, ethane and carbon dioxide  
23  
24 (compounds known to be present on the Titan surface) and other organics (like ethylene and  
25  
26 many others) can provide significant acoustic absorption at the frequencies discussed.  
27  
28  
29  
30  
31

32  
33  
34  
35  
36 Niemann et al. (2005; 2010) show that the GCMS instrument detected several species after  
37  
38 landing (see figure 10). Note that there is no expectation of an exact correspondence between  
39  
40 the GCMS readings and the gas abundances in the SSP cavity since the thermal histories of  
41  
42 whatever material was jammed into the heated GCMS inlet and the possibility of evaporation  
43  
44 of dampness around it and its diffusion into the gas sampling tubes may have been quite  
45  
46 different from the warming of any material scraped into the SSP cavity or warmed underneath  
47  
48 the probe. However, the overall timeline is probably representative - e.g. figure 11 shows the  
49  
50 warming of the interior of the top hat, and the corresponding dew point of the ethane partial  
51  
52 pressure measured by GCMS (which should be seen only as representative, since the  
53  
54  
55  
56  
57  
58  
59  
60  
61  
62  
63  
64  
65

1  
2  
3  
4  
5  
6 temperature evolutions of GCMS and SSP would not have been identical, and the ethane vapor  
7  
8 pressure may have been influenced by other solutes in the damp ground).  
9

10  
11 The saturation vapor pressure of pure ethane is very small (equivalent to a mixing ratio of  
12  
13 about 30ppm at Titan's surface temperature of 94K) but rises steeply with temperature. Should  
14  
15 surface material damp with ethane have warmed to 120-140K, the saturation mixing ratio  
16  
17 would increase to 0.2-2%. The GCMS data show that several other compounds rose in detected  
18  
19 abundance over an hour or so after landing. Benzene and cyanogen were detected, and so it  
20  
21 seems likely that a rich cocktail of hydrocarbons and nitriles (and, indeed, CO<sub>2</sub>, a well-known  
22  
23 acoustic absorber) may have similarly accumulated in the top hat cavity.  
24  
25  
26  
27  
28  
29  
30  
31  
32

33  
34 Leese et al. (2012) noted that during API-V Specific to Experiment Test on the flight model  
35  
36 probe, which involved using a purpose built Top Hat non-flight cover to introduce several  
37  
38 different gases and flush through the Top Hat cavity for each, carbon dioxide produced  
39  
40 timeouts (i.e. no signal detected) for very low concentrations in nitrogen due to high acoustic  
41  
42 absorption. In addition to this well-known effect of the pure gas, Garry (1996) noted in ground  
43  
44 tests of the API-V system that an order of magnitude drop in signal was encountered when  
45  
46 purging a test cavity with nitrogen after making measurements in ethane or methane. This  
47  
48 transient attenuation due to nitrogen/methane or nitrogen/ethane mixtures could not be  
49  
50 characterized in detail, unfortunately, since no means was available to measure the changing  
51  
52 composition. Thus we call attention to the need for quantitative acoustic absorption  
53  
54 measurements of nitrogen mixtures with other gases, at temperatures of around 100K.  
55  
56  
57  
58  
59  
60  
61  
62  
63  
64  
65

1  
2  
3  
4  
5  
6  
7  
8  
9 < Figure 10 >

10  
11  
12 < Figure 11 >

13  
14  
15  
16  
17  
18  
19 The statistical behavior of the lost pulses is interesting, in that bursts of pulses appear to break  
20 through above the detection threshold - e.g. at 9800-9900s, these bursts are 5-10s long,  
21  
22 whereas later, at 10000s (see figure 12) the bursts are more like 20s. Furthermore, when  
23  
24 propagation is successful in one direction (e.g. T1) it is often also successful in the other,  
25  
26 suggesting a common factor. One possibility might be that the gas supply and/or removal is  
27  
28 discretized somehow, e.g. bubbles of gas released from the subsurface like a plopping mudpot.  
29  
30 There is unfortunately little data to constrain such speculation, although any subsurface  
31  
32 phenomena were evidently too weak to cause any disturbance measurable by the sensitive  
33  
34 accelerometers and tiltmeters on the probe.  
35  
36  
37  
38  
39  
40  
41  
42  
43  
44  
45  
46

47 < Figure 12 >

## 48 49 50 51 52 53 5. Conclusions

54  
55  
56  
57 The speed-of-sound instrument, whose principal intended role on the payload was to measure  
58  
59 the properties of Titan's seas, nonetheless provided some information during descent and after  
60  
61  
62  
63  
64  
65

1  
2  
3  
4  
5 landing, and suggests that sound propagation was suppressed about 20 minutes after  
6  
7  
8 touchdown.  
9

10  
11 Clearly, using the function of a threshold detector in this way is not an ideal attenuation  
12  
13 measurement, having a very modest dynamic range. Nonetheless, the most plausible  
14  
15 interpretation of the cessation of signals post-landing is the evolution of absorbing vapors from  
16  
17 the surface. This independent detection of volatiles reinforces the notion that the surface  
18  
19 materials at the landing site were 'damp', and underscores that unexpected results can be  
20  
21 obtained from acoustic instrumentation. We may recall the words of Charlotte Bronte "Silence  
22  
23 is of different kinds, and breathes different meanings."  
24  
25  
26  
27  
28  
29

30  
31 One lesson is that the interpretation of a notionally-simple instrument in an unknown  
32  
33 environment was rather complex. A housekeeping measurement of signal strength, even on a  
34  
35 small subset of the measurements, would have greatly assisted interpretation. More  
36  
37 ambitiously, the ability to measure at a range of frequencies - to conduct acoustic absorption  
38  
39 spectroscopy - might permit identification of the absorbing gases. Of course on future Titan  
40  
41 missions any such augmented capabilities would be in competition with a range of other  
42  
43 scientific experiments and so the richness and significance of findings that might result must be  
44  
45 traded off against the resource requirements and the opportunity costs of other types of  
46  
47  
48  
49 instrumentation.  
50  
51  
52  
53  
54  
55  
56  
57

## 58 6. Acknowledgements 59 60 61 62 63 64 65

1  
2  
3  
4  
5  
6 Cassini-Huygens is a joint endeavour of NASA, ESA and ASI. The results reported here were  
7  
8 made possible by the efforts of many colleagues on the Huygens team. RL acknowledges the  
9  
10 support of the Cassini project at the Jet Propulsion Laboratory, via NASA grant NNX13AH14G.  
11  
12  
13 The lead author acknowledges useful discussions on acoustics with Juan Arvelo of APL and Tim  
14  
15  
16 Leighton of the University of Southampton.  
17  
18  
19  
20  
21  
22  
23  
24  
25  
26  
27  
28  
29  
30  
31  
32  
33  
34  
35  
36  
37  
38  
39  
40  
41  
42  
43  
44  
45  
46  
47  
48  
49  
50  
51  
52  
53  
54  
55  
56  
57  
58  
59  
60  
61  
62  
63  
64  
65

## References

- Bettanini, C., Zaccariotto, M., Angrilli, F., 2008. Analysis of the HASI accelerometers data measured during the impact phase of the Huygens probe on the surface of Titan by means of a simulation with a finite element model. *Planetary and Space Science* 56, 715–727.
- Dain, Y. and R. M. Lueptow, 2001. Acoustic Attenuation in a three-gas mixture: Results, *J. Acoustical Society of America*, 110, 2974-2979
- Ejakov, S. G. Acoustic attenuation in gas mixtures with nitrogen : Experimental data and calculations, *J. Acoustical Society of America*, 113, 1871-1879
- Garry, J.R.C., 1996. Surveying Titan Acoustically. MSc Thesis, University of Kent at Canterbury, Canterbury. (Garry, J.R.C., Kent, M.Sc., 1996, C3 46-9855).
- Hagermann, A., P.D. Rosenberg, M.C. Towner, J.R.C. Garry, H. Svedhem, M.R. Leese, B. Hathi, R.D. Lorenz, J. C. Zarnecki, 2007. Speed of sound measurements and the methane abundance in Titan's atmosphere, *Icarus*, 189, 538-543
- Hanford, A. D. and L. N. Long, 2009. The direct simulation of acoustics on Earth, Mars and Titan, *J. Acoustical Society of America*, 125, 640-650
- Holmes, R., G. R. Jones and N. Pusat, 1964. Vibrational Relaxation in Propane, Propylene and Ethane, *Journal of Chemical Physics*, 41, 2512-2516

1  
2  
3  
4  
5  
6 Karkoschka, E., Tomasko, M.G., Doose, L.R., See, C., McFarlane, E.A., Schroeder, S.E., Rizk, B.,  
7  
8 2007. DISR imaging and the geometry of the descent of Huygens. Planetary and Space Science  
9  
10 55, 1896–1935.

11  
12  
13  
14 Karkoschka, E., Tomasko, M.G 2009. Rain and dewdrops on titan based on in situ imaging,  
15  
16 Icarus, 199, 442-448  
17  
18

19  
20  
21  
22  
23  
24 Leese, M. R., R. D. Lorenz, B. Hathi and J. C. Zarnecki, 2012. The Huygens Surface Science  
25  
26 Package (SSP): Flight Performance Review and Lessons Learned, Planetary and Space Science,  
27  
28 70, 28-45  
29  
30

31  
32 Leighton, T. G. and White, P. R.,2004. The Sound of Titan - a role for acoustics in space  
33  
34 exploration, Acoust. Bull. 16-23  
35  
36

37  
38 Leighton, T.G. and Petculescu, A. 2009. The sound of music and voices in space, Acoustics  
39  
40 Today, 5, 17-29  
41  
42

43  
44 Lorenz, R. D. 1994. Exploring the Surface of Titan, Ph.D. Thesis, University of Kent at Canterbury  
45  
46

47  
48 Lorenz, R. D., 2006. Thermal Interaction of the Huygens Probe with the Titan Environment :  
49  
50 Surface Windspeed Constraint, Icarus, 182, 559-566  
51  
52

53  
54 Lorenz, R. D., H. Niemann, D. Harpold, J. Zarnecki, Titan's Damp Ground : Constraints on Titan  
55  
56 Surface Thermal Properties from the Temperature Evolution of the Huygens GCMS inlet, 2006.  
57  
58 Meteoritics and Planetary Science. 41, 1405-1414  
59  
60  
61  
62  
63  
64  
65

- 1  
2  
3  
4  
5 Lorenz, R. D., J. C. Zarnecki, M. C. Towner, M. R. Leese, A. J. Ball, B. Hathi, A. Hagermann, N. A.  
6  
7  
8 L. Ghafoor, 2007. Descent Motions of the Huygens Probe as Measured by the Surface Science  
9  
10 Package (SSP) : Turbulent Evidence for A Cloud Layer, *Planetary and Space Science*, 55, 1936-  
11  
12 1948  
13  
14  
15  
16 Lorenz, R. D., 2007. Titan Atmosphere Profiles from Huygens Engineering (Temperature and  
17  
18 Acceleration) Sensors, *Planetary and Space Science*, 55, 1949-1958  
19  
20  
21  
22  
23 Martinsson, P.-E., and J. Delsing, 2002. Ultrasonic Measurements of Molecular Relaxation in  
24  
25 Ethane and Carbon Monoxide, pp.511-515 in *Proceedings, 2002 IEEE Ultrasonics Symposium*.  
26  
27  
28  
29 Niemann, H.B., Atreya, S.K., Bauer, S.J., Carignan, G.R., Demick, J.E., Frost, R.L., Gautier, D.,  
30  
31 Haberman, J.A., Harpold, D.N., Hunten, D.M., Israel, G., Lunine, J.I., Kasprzak, W.T., Owen, T.C.,  
32  
33 Paulkovich, M., Raulin, F., Raaen, E., Way, S.H., 2005. The abundances of constituents of Titan's  
34  
35 atmosphere from the GCMS instrument on the Huygens probe. *Nature* 438, 779–784.  
36  
37  
38  
39 Niemann, H. B., S. K. Atreya, J. E. Demick, D. Gautier, J. A. Haberman, D. N. Harpold, W. T.  
40  
41 Kasprzak, J. I. Lunine, T. C. Owen, and F. Raulin, 2010. Composition of Titan's lower atmosphere  
42  
43 and simple surface volatiles as measured by the Cassini-Huygens probe gas chromatograph  
44  
45 mass spectrometer experiment, *Journal of Geophysical Research*, 115, E12006,  
46  
47  
48  
49 doi:10.1029/2010JE003659  
50  
51  
52  
53 Pérez-Ayúcar M., Lorenz R. D., Flourey N., Prieto R., Lebreton J.-P., 2006. Surface Properties of  
54  
55 Titan from Post-Landing Reflections of the Huygens Radio Signal, *JGR – Planets*, 111, E07001,  
56  
57  
58  
59 doi:10.1029/2005JE002613  
60  
61  
62  
63  
64  
65



1  
2  
3  
4  
5  
6 Petelescu, A., B. Hall, R. Fraenzle, S. Phillips, R. M. Lueptow, 2006. A prototype acoustic gas  
7  
8 sensor based on attenuation, *J. Acoustical Society of America*, 120, 1779-1782  
9

10  
11 Petculescu, A. and P. Achi, 2012. A model for the vertical sound speed and absorption profiles  
12  
13 in Titan's atmosphere based on Cassini-Huygens data, *J. Acoustical Society of America*, 131,  
14  
15 3671-3679  
16  
17

18  
19  
20 Petculescu, A. and R. M. Lueptow, 2007. Atmospheric acoustics of Titan, Mars, Venus, and  
21  
22 Earth, *Icarus*, 186, 413-319  
23  
24  
25

26 Rosenberg, P.D., 2007. Huygens' Measurements of the Speed of Sound on Titan. PhD Thesis,  
27  
28 The Open University, Milton Keynes. (An EThOS/ BL Reference number for the 2008 thesis by  
29  
30 Rosenberg, P.D. is DXN116951)  
31  
32

33  
34  
35 Schroeder, S. E., E. Karkoschka and R. D. Lorenz, 2012. Bouncing on Titan : Motion of the  
36  
37 Huygens Probe in the seconds after landing, *Planetary and Space Science*, 73, 327-340  
38  
39

40  
41 Svedhem, H., Lebreton, J.-P., Zarnecki, J.C., Hathi, B., 2004. Using speed of sound  
42  
43 measurements to constrain the Huygens probe descent profile. *ESA SP-544*, 221–228.  
44  
45  
46  
47  
48  
49  
50  
51  
52  
53  
54  
55  
56  
57  
58  
59  
60  
61  
62  
63  
64  
65

1  
2  
3  
4  
5  
6  
7  
8  
9 Towner, M. C., J.R.C. Garry, R.D. Lorenz, B. Hathi, A. Hagermann, H. Svedhem, B.C. Clark, M.R.

10  
11 Leese, J.C. Zarnecki, 2006. Physical properties of the Huygens landing site from the Surface

12  
13 Science Package Acoustic Properties sensor (API S), Icarus, 185, 457-465

14  
15  
16  
17 Zarnecki, J.C., Banaszkiwicz, M., Bannister, M., Boynton, W.V., Challenor, P., Clark, B., Daniell,

18  
19 P.M., Delderfield, J., English, M.A., Garry, J.R.C., Geake, J.E., Green, S.F., Hathi, B., Jaroslowski,

20  
21 S., Leese, M.R., Lorenz, R.D., McDonnell, J.A.M., Merryweather-Clarke, N., Mill, C.S., Miller, R.J.,

22  
23  
24  
25 Newton, G., Parker, D.J., Svedhem, H., Wright, M.J., 1997. The Huygens Surface Science

26  
27 Package. In: Wilson, A. (Ed.), Huygens: Science, Payload and Mission. ESA SP-1177. ESA

28  
29 Publications Division, Noordwijk, pp. 177–195.

30  
31  
32  
33 Zarnecki, J.C., Leese, M.R., Garry, J.R.C., Ghafoor, N., Hathi, B., 2002. Huygens' Surface Science

34  
35  
36  
37 Package. Space Sci. Rev., 104, 593–611.

38  
39  
40 Zarnecki, J.C., Leese, M.R., Hathi, B., Ball, A.J., Hagermann, A., Towner, M.C., Lorenz, R.D.,

41  
42 McDonnell, J.A.M., Green, S.F., Patel, M.R., Ringrose, T.J., Rosenberg, P.D., Atkinson, K.R.,

43  
44  
45 Paton, M.D., Banaszkiwicz, M., Clark, B.C., Ferri, F., Fulchignoni, M., Ghafoor, N.A.L., Kargl, G.,

46  
47  
48 Svedhem, H., Delderfield, J., Grande, M., Parker, D.J., Challenor, P.G., Geake, J.E., 2005. A soft

49  
50 solid surface on Titan at the Huygens landing site as measured by the Surface Science Package

51  
52  
53 (SSP). Nature 438 (7069), 792795.

54  
55  
56  
57  
58  
59  
60  
61  
62  
63  
64  
65

## Figure Captions

Figure 1. Location of the SSP API-V sensors on the underside of the Huygens probe, with the anti-static screen shown displaced downwards for clarity.

Figure 2 . View of the SSP 'Top Hat' structure with the grill removed. The metallic boxes at top and bottom are the API-V speed of sound transducer housings (the circular transducer surface is just visible on the right one). The penetrometer is visible at left (note also the grounding strap) and the acoustic sounder at lower right.

Figure 3. The metal grill shown in position on the front of the SSP Top Hat. Most photographs of the probe show the instrumentation with the grill removed, but it is important in understanding the possible influences on the acoustic instrumentation.

Figure 4. The API-V data against mission time. The 'good' propagation times (A) measured during the lower part of descent have been analyzed in detail by Hagermann et al. (2007). Surface measurements (B) are discussed in the present paper. For most of the descent, the receive pulse threshold was not crossed and the counter timed out, forming two clouds of points (C, D) - the timeout was different for the two propagation directions. A spurious set of early triggers (E) are present and are discussed in the text and may be related to noise from the Aerosol Collector Pyrolyzer (ACP) pump.

Figure 5. Statistics of T2 propagation times in 200s blocks leading up to landing (dataset A in figure 4). Initially (6650s, about 14km) there are no received pulses and only timeouts at

1  
2  
3  
4  
5  
6 ~0.78ms are present. As the probe descends into denser air, propagated pulses begin to appear  
7  
8 correctly at ~0.7ms and progressively dominate, with almost no timeouts present after ~8000s,  
9  
10  
11 until the last 1km of descent. Why this should occur is not clear.  
12  
13

14 Figure 6. Statistics of propagation times (x-axis, milliseconds) in 200-second blocks of data  
15  
16 after landing (dataset B in figure 4). The right-hand peaks (>0.72 ms) correspond to timeouts,  
17  
18 the left hand peak to valid pulse receipt. Data start 30s after the impact at 8870s - it is known  
19  
20 that the probe was still moving for a few seconds after contact. Initially (8900-9100s) there are  
21  
22 no clean pulses, perhaps as a result of material adhering to the transducers. Over 9100-9500s a  
23  
24 good strong signal builds up and the proportion of timeouts declines, but then increases again  
25  
26  
27 over 9500-10300s, with no further clean pulses getting through thereafter. Notice also that  
28  
29 while at 9100s-9300s the 'good' pulse histogram is sharp indicating clean triggers from a strong  
30  
31 signal, the histogram for 9700s and thereafter is broader and positively skewed, i.e. with a  
32  
33 fraction of 'late' triggers. As discussed in Hagermann et al. (2007) this is a signature of a weak  
34  
35  
36  
37  
38  
39  
40  
41  
42  
43  
44  
45  
46  
47  
48  
49  
50  
51  
52  
53  
54  
55  
56  
57  
58  
59  
60  
61  
62  
63  
64  
65

Figure 7. 200-sample running mean of the fraction of good pulses (i.e. transit times in the valid range of 0.6 to 0.7 ms) in the two directions (T1, T2) just after landing. In fact the performance jumps rapidly upwards after landing (the 200-sample smoothing limits the gradient, but shows better the quantitative decline in performance after 9500s).

1  
2  
3  
4  
5  
6 Figure 8. Dimensionless attenuation of several gases mixed with nitrogen. The Huygens API-V  
7  
8 measurement on the surface corresponds to  $f/P=6E5$  Hz/bar, rather close to where the  
9  
10 ethylene absorption has a peak. Curves extracted from Petelescu et al. (2006) and Dain and  
11  
12 Lueptow (2001).  
13  
14  
15

16  
17 Figure 9. Dimensionless attenuation for several gas mixtures. Note the very strong absorption  
18  
19 by  $CO_2$ , although this peaks at a frequency an order of magnitude lower than that for ethylene  
20  
21 ( $C_2H_4$ ). Curves extracted from Petelescu et al. (2006) and Dain and Lueptow (2001).  
22  
23  
24

25  
26 Figure 10. The mixing ratio evolution of some acoustically-absorbing gases sampled by the  
27  
28 Huygens GCMS (Niemann et al., 2010). The rise post-impact is due to heating of the inlet,  
29  
30 embedded in the surface material.  
31  
32

33  
34 Figure 11. Temperature evolution of the PERmittivity sensor near the front of the top hat.  
35  
36 Although formally unrelated, the dew point of the ethane partial pressure indicated by the  
37  
38 GCMS is also shown, illustrating the broad consistency between the rise of probe-base  
39  
40 temperatures and the presence of volatiles. The period in which the pulse transit efficiency  
41  
42 declines to zero is indicated, and corresponds with the rise in volatile abundance.  
43  
44  
45  
46  
47  
48  
49  
50  
51  
52  
53  
54  
55  
56  
57  
58  
59  
60  
61  
62  
63  
64  
65

1  
2  
3  
4  
5  
6 Figure 13. Time series of data (essentially a zoom of figure 4) as the overall propagation  
7  
8 probability was declining on the surface. Valid data tends to appear in bursts in both directions,  
9  
10 here around 20s long, with T2 tending to fail more often.  
11  
12  
13  
14  
15  
16  
17  
18  
19  
20  
21  
22  
23  
24  
25  
26  
27  
28  
29  
30  
31  
32  
33  
34  
35  
36  
37  
38  
39  
40  
41  
42  
43  
44  
45  
46  
47  
48  
49  
50  
51  
52  
53  
54  
55  
56  
57  
58  
59  
60  
61  
62  
63  
64  
65

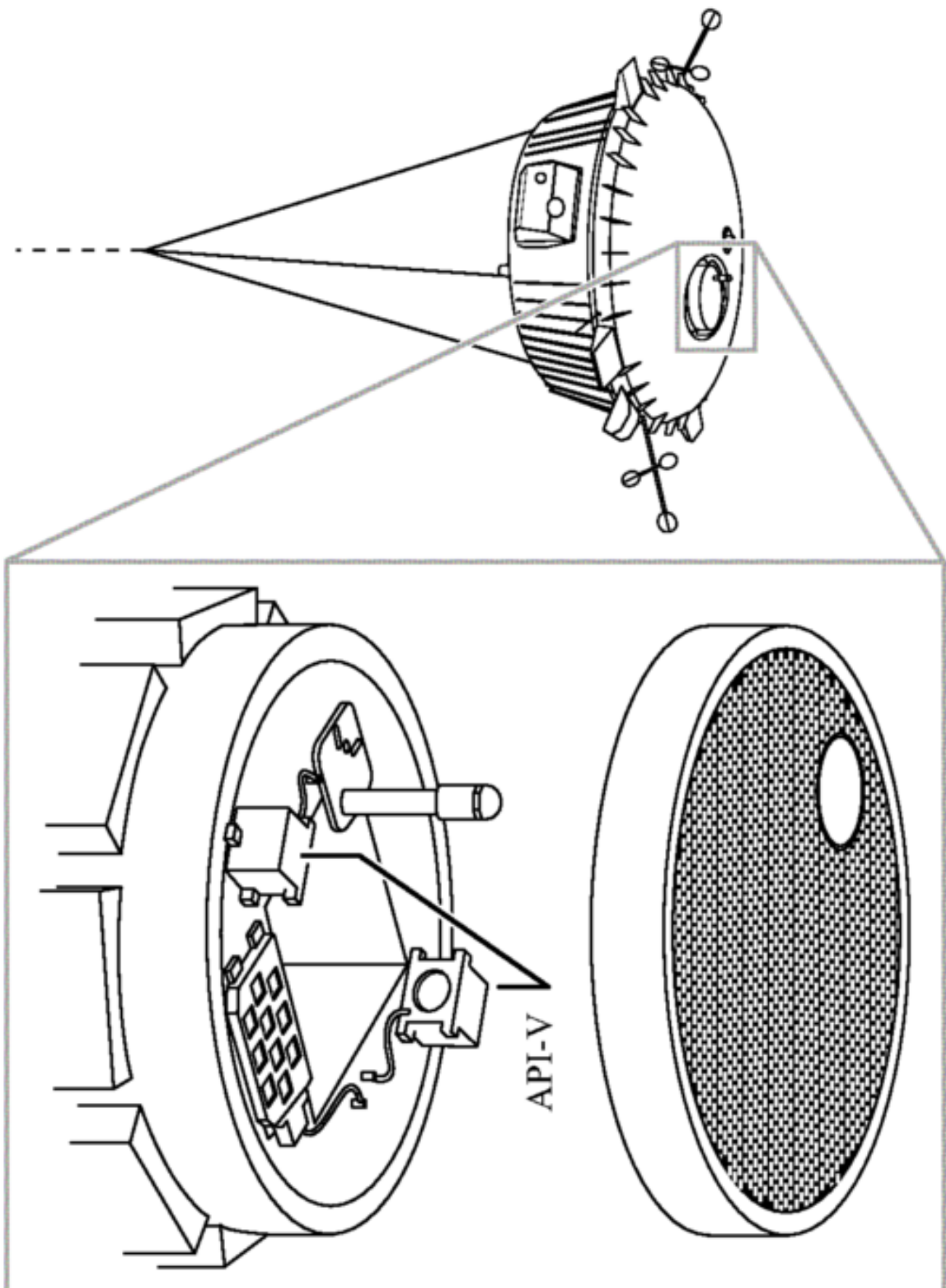


Figure  
[Click here to download high resolution image](#)

Figure  
[Click here to download high resolution image](#)





Figure  
[Click here to download high resolution image](#)



Figure  
[Click here to download high resolution image](#)

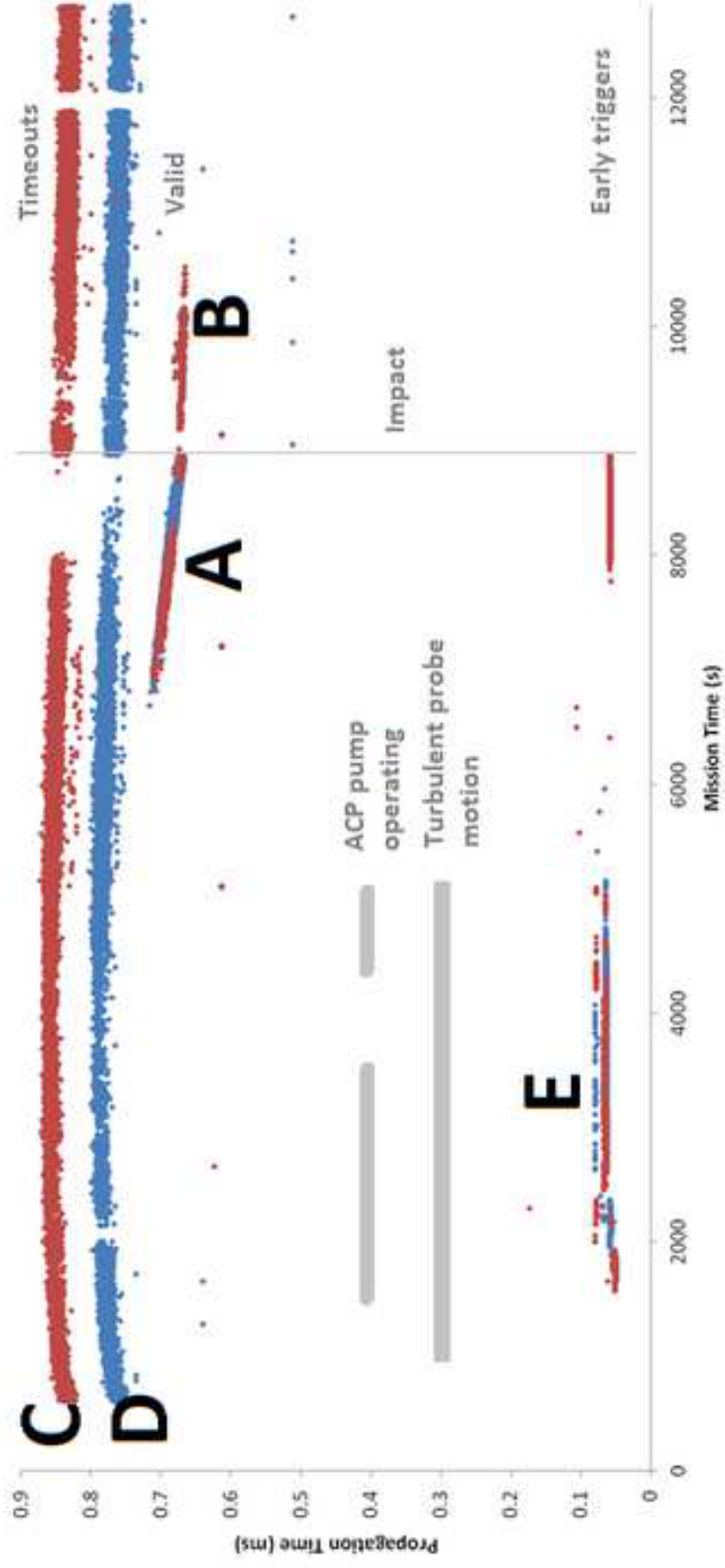


Figure  
[Click here to download high resolution image](#)

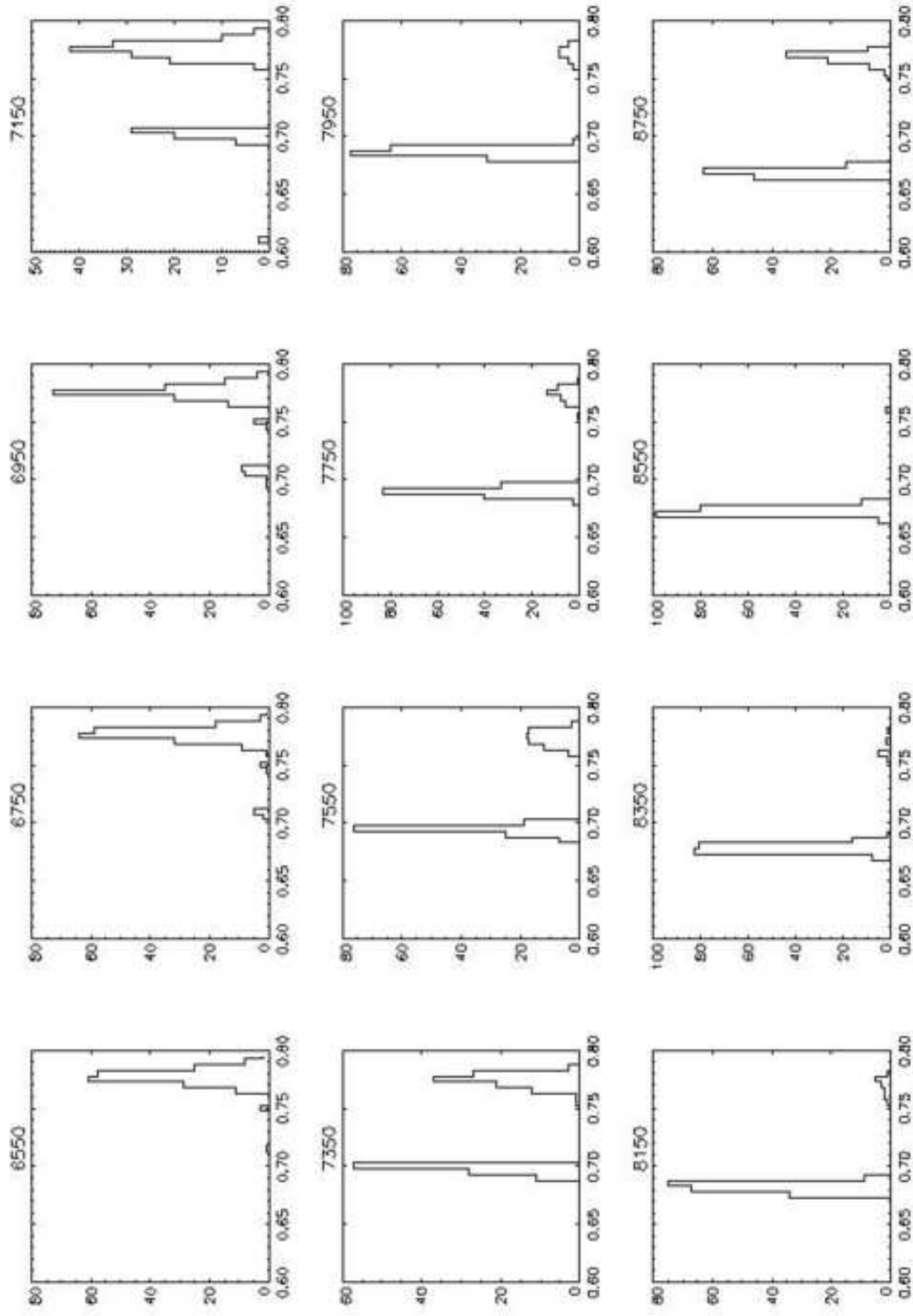


Figure  
[Click here to download high resolution image](#)

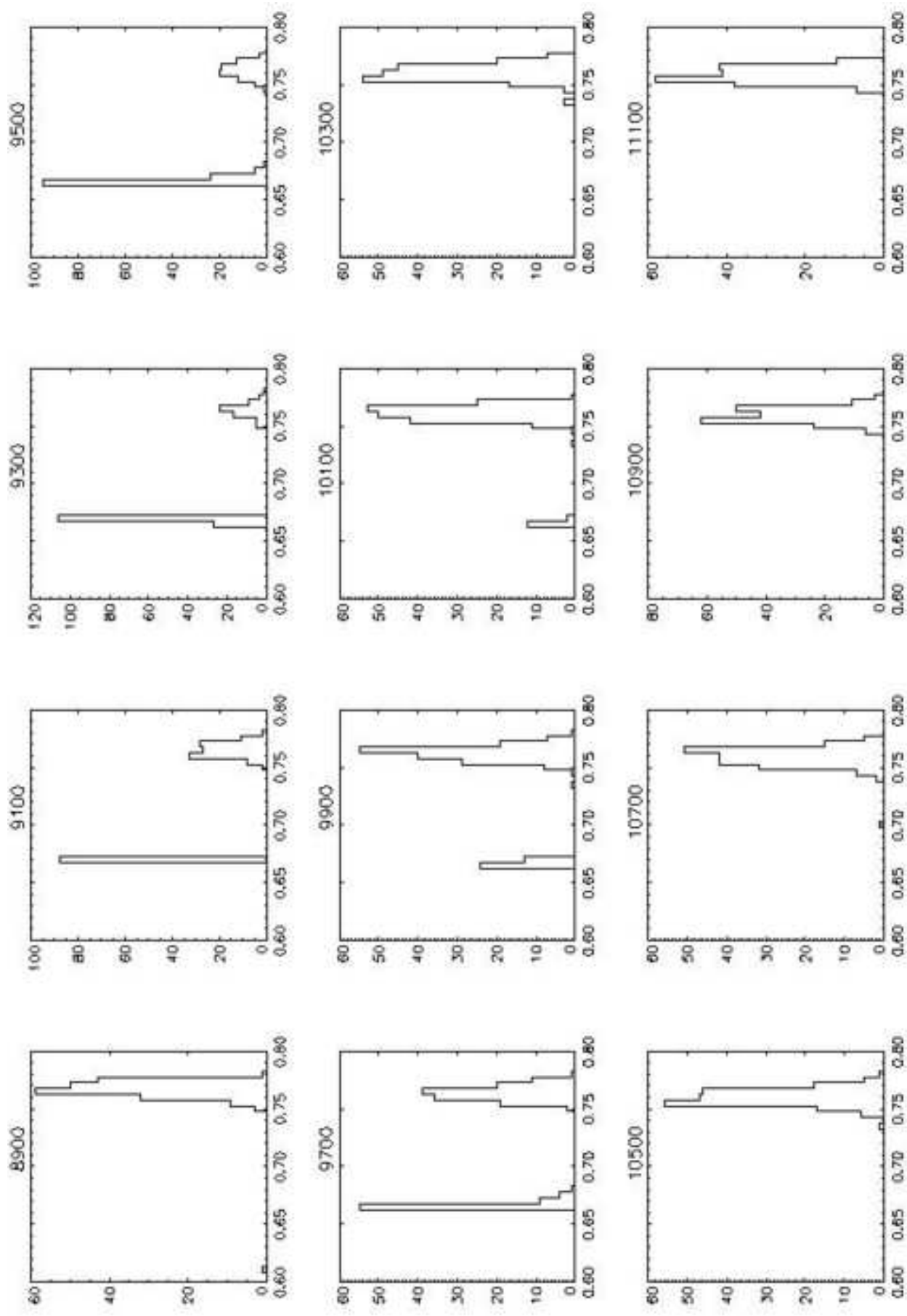
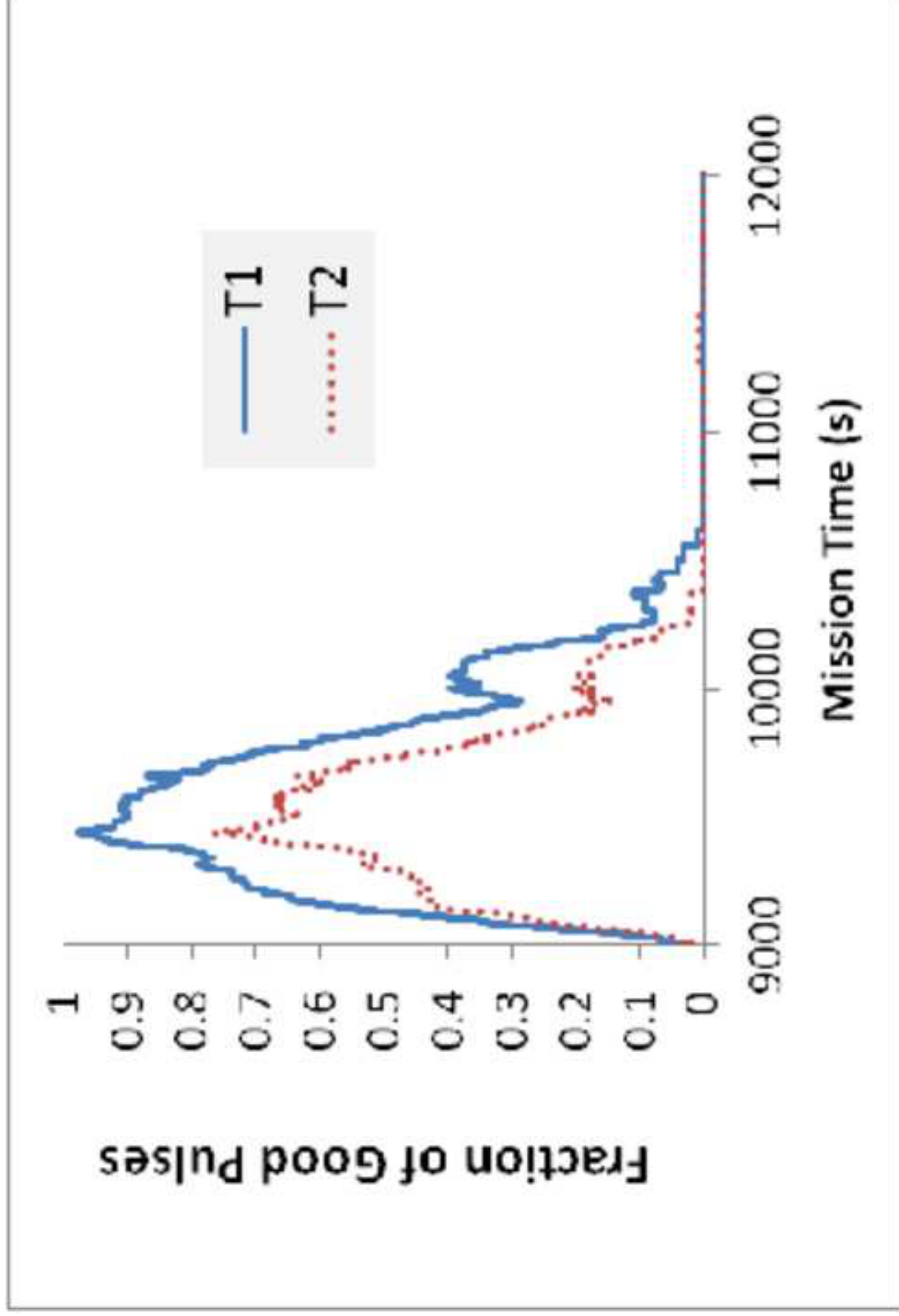


Figure  
[Click here to download high resolution image](#)



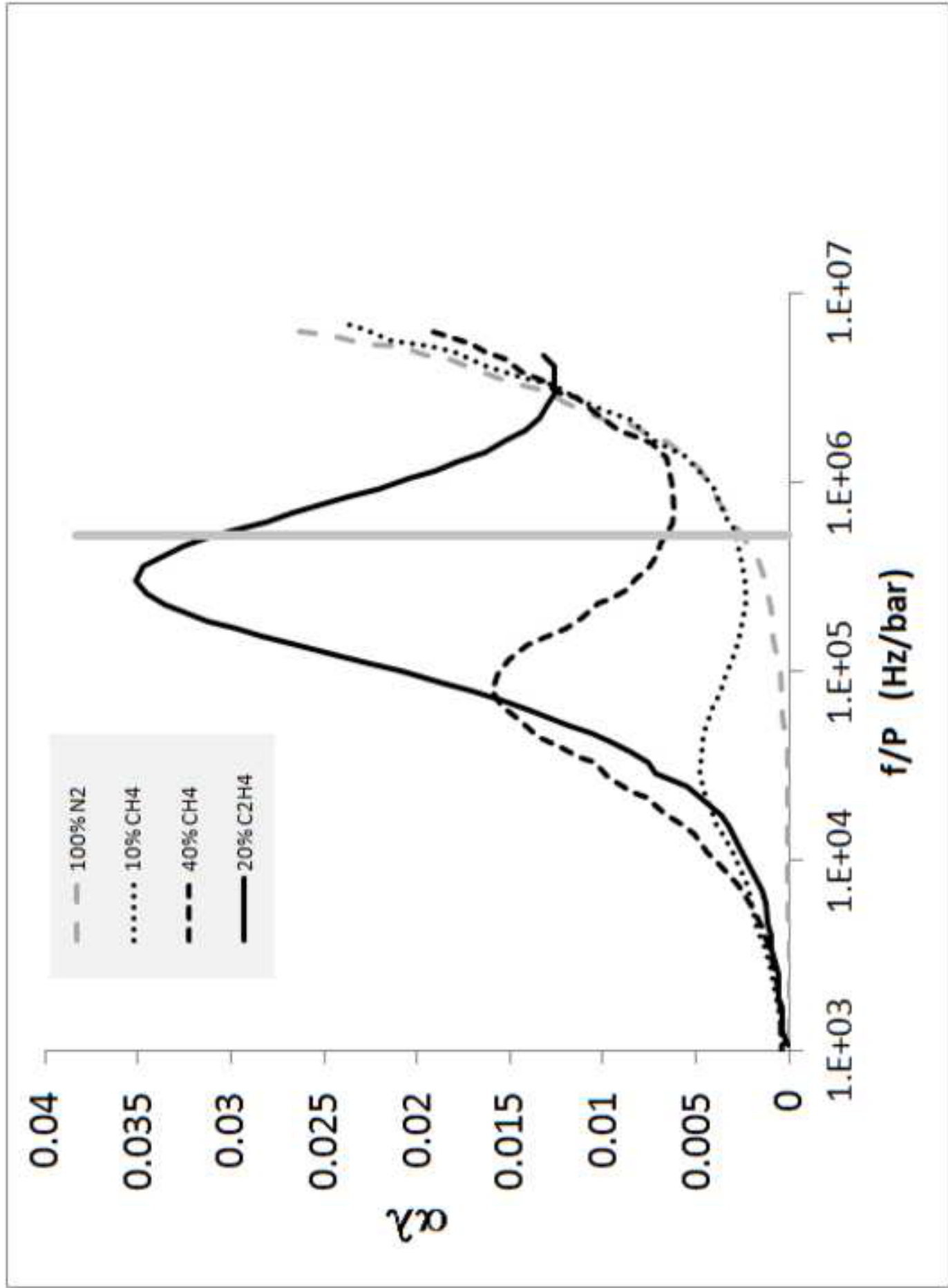


Figure  
[Click here to download high resolution image](#)

Figure  
[Click here to download high resolution image](#)

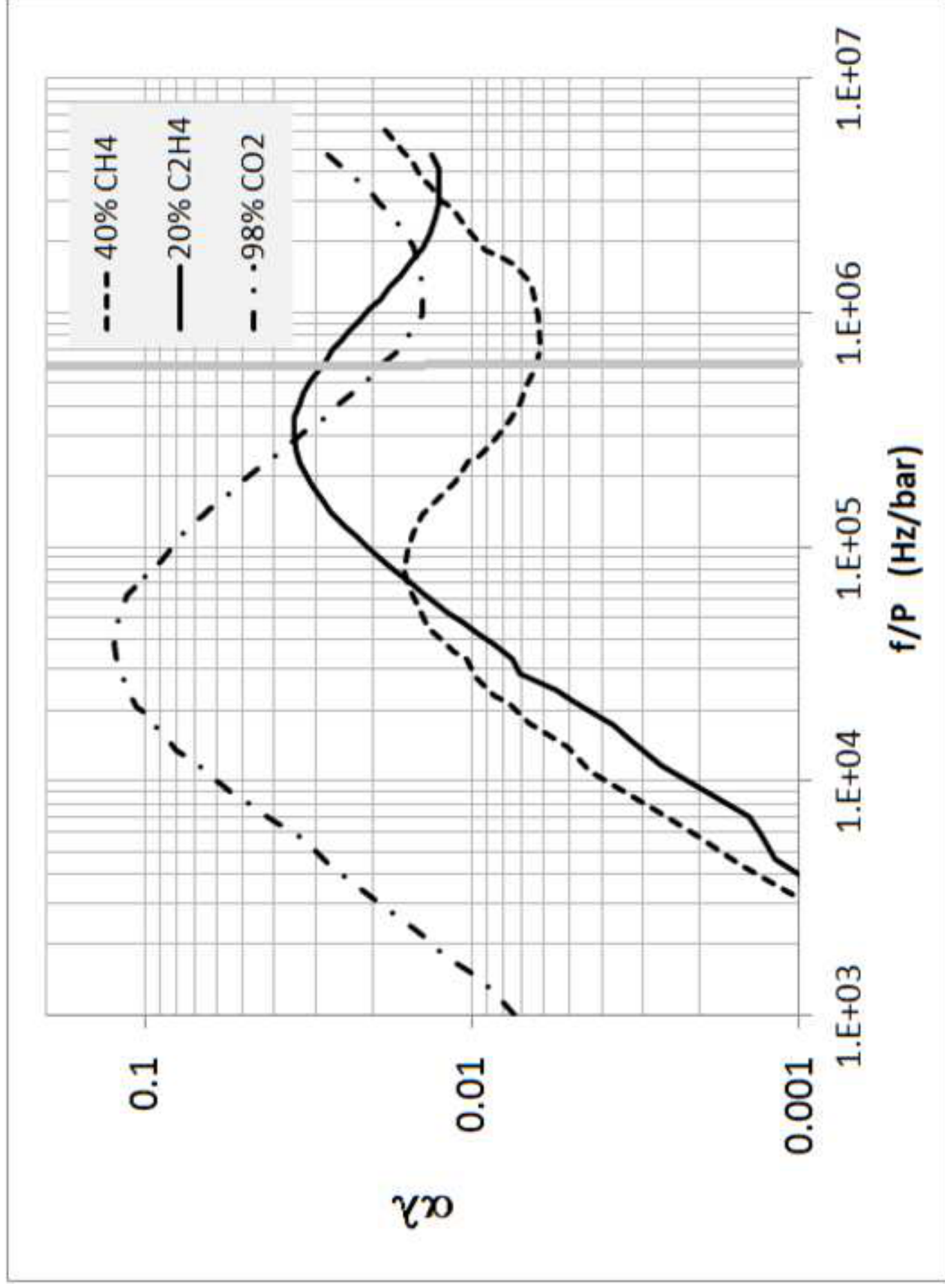


Figure  
[Click here to download high resolution image](#)

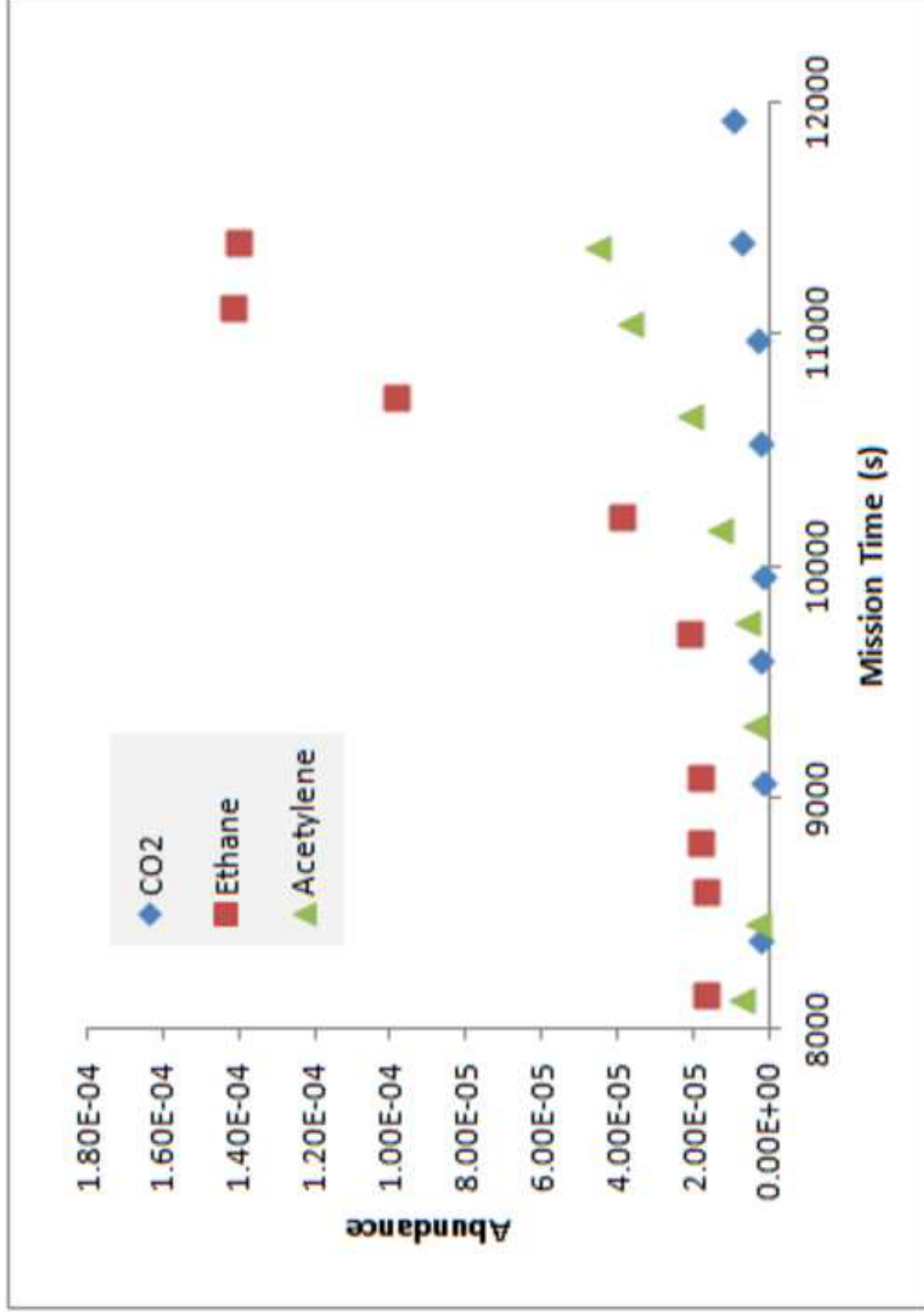
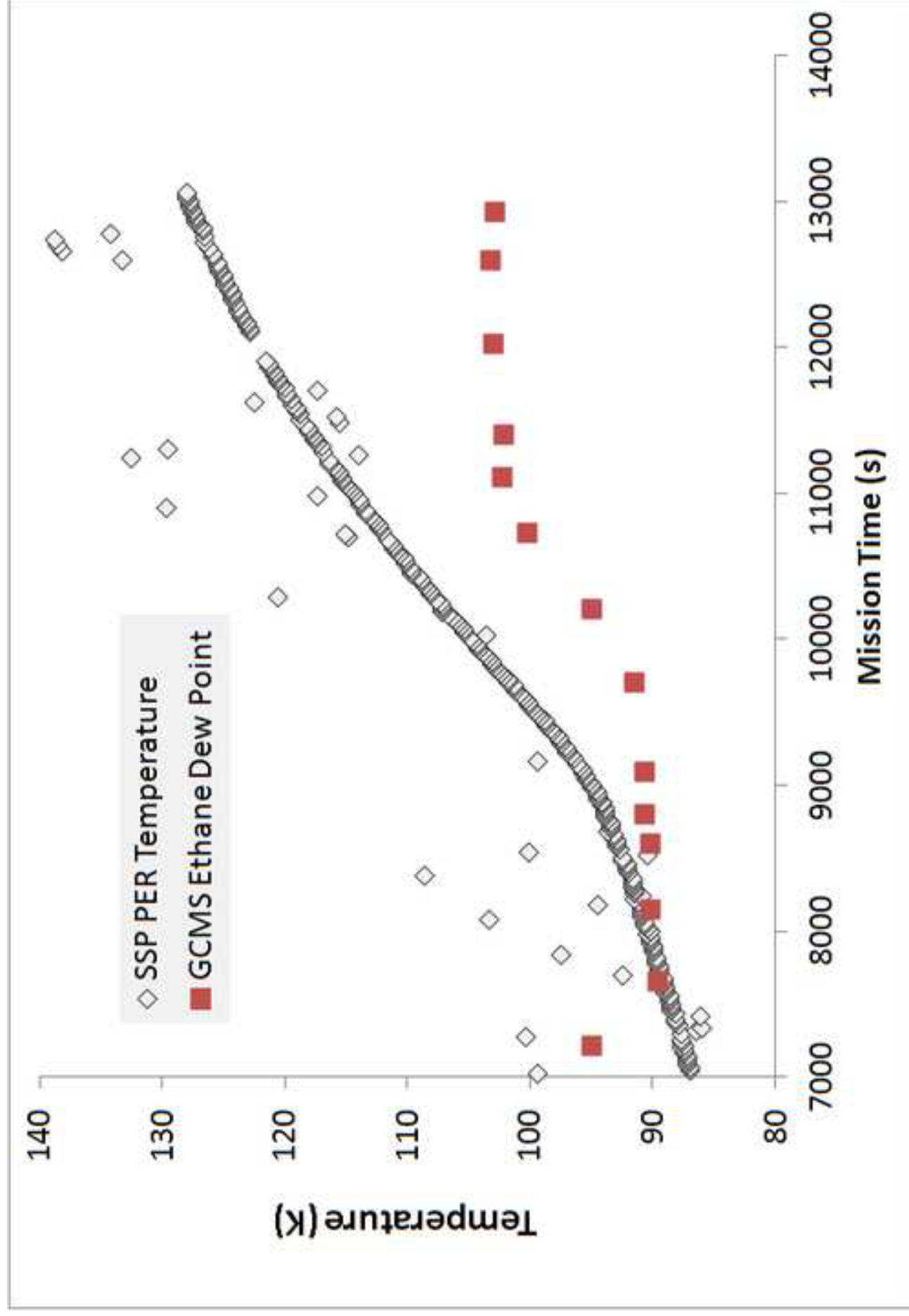




Figure  
[Click here to download high resolution image](#)



Figure

[Click here to download high resolution image](#)

